Journal of Photochemistry and Photobiology A: Chemistry 201 (2009) 157–167

Contents lists available at ScienceDirect

Journal of Photochemistry and Photobiology A: Chemistry

journal homepage: www.elsevier.com/locate/jphotochem

# Triplet-sensitized photolysis of alkoxycarbonyl azides in solution and matrices

Rajesh S. Murthy, Sivaramakrishnan Muthukrishnan, Sridhar Rajam, Sarah M. Mandel, Bruce S. Ault, Anna D. Gudmundsdottir*

*Department of Chemistry, University of Cincinnati, Cincinnati, OH 45221-0172, USA*

ARTICLE INFO

*Article history:*
Received 13 August 2008
Received in revised form 6 October 2008
Accepted 22 October 2008
Available online 6 November 2008

*Keywords:*
Ester nitrenes
Laser flash photolysis
Matrix isolation
DFT calculation

ABSTRACT

Photolysis of azides **1**–**4** in methanol, which have a built-in intramolecular triplet sensitizer, yields mainly carbamates **5**–**8**. Laser flash photolysis of **1**–**4** shows formation of their triplet-excited ketone, which decays by intramolecular energy transfer to form triplet nitrenes **1n**–**4n**. Irradiating **1**–**3** in matrices yields isocyanic acid, whereas photolysis of **4** forms isocyanate **4i**. The depletion rate of the azide bands between 2100 and 2200 $cm^{-1}$ is different than the rate of formation for the isocyanic acid bands at ~2265 $cm^{-1}$; thus, the formation of isocyanic acid is a stepwise process. Irradiating **1** in matrices produces an absorption band due to nitrene **1n** ($\lambda_{max}$ ~ 343 nm), which is depleted upon further irradiation, whereas the absorption due to 4-acetyl benzaldehyde ($\lambda_{max}$ ~ 280 nm) increases with prolonged irradiation. We propose that formation of isocyanic acid in matrices must come from secondary photolysis of nitrenes **1n**–**3n**. This mechanism is further supported by calculation, which show that the estimated transition state for **1n**–**4n** to fall apart to yield alkoxy and cyanato radicals is only ~34 kcal/mol above the ground state of the triplet nitrenes and thus the cleavage can take place photochemically. Thus, nitrenes **1n**–**4n** can be formed selectively, but these intermediates are highly photosensitive and undergo secondary photolysis in matrices.



## 1. Introduction

Carboalkoxy nitrene intermediates are highly reactive, making them useful in processes such as crosslinking polymers and photoaffinity labelling [1]. For example, the indiscriminate insertion of the singlet carboalkoxy nitrene into C–C bonds has been used to functionalize nanotubes [2]. Lwowski et al. first demonstrated that photolyzing carbonazidic acid ethyl ester in cyclohexene yields mainly compounds that can be attributed to the formation of singlet carboethoxy nitrene, which inserts into the C–C and the C–H bonds of the solvent [3]. Lwowski et al. also studied the reactivity of carboethoxy nitrene with cis- and trans-4-methyl-2-pentene as a function of the alkene concentration, and found that the carboethoxy nitrene addition to the double bond is stereospecific only at high concentrations of alkene [4]. The authors concluded that singlet carboethoxy nitrene is produced initially, but subsequently relaxes to triplet carboethoxy nitrene, which adds to the double bond in a stepwise, non-stereospecific mechanism. Thus, triplet carboethoxy nitrene has been assigned as the ground state of carboethoxy nitrenes. Photolysis of carbonazidic acid ethyl ester at low temperature further supports that the triplet is the ground state, since it gives rise to EPR signals assignable to the formation of triplet carboethoxynitrene [5]. Calculations confirm that the triplet carboethoxy nitrene is between 3 and 8 kcal/mol lower in energy than the singlet [6–9]. Recently, Buron and Platz detected triplet carboethoxy nitrenes directly with laser flash photolysis of carbonazidic acid ethyl ester and estimated the rate of intersystem crossing from the singlet to triplet nitrene to be on the order of $10^8$ $s^{-1}$ [6].

In contrast, Lwowski and coworkers demonstrated that photolysis of carbonazidic acid methyl ester in matrices yields methoxy isocyanate, which reacts further to produce isocyanic acid [10]. It was concluded that the excited state of carbonazidic acid methyl ester, rather than the singlet carbomethoxy nitrene, undergoes a Curtius rearrangement to form the methoxy isocyanate, since no intermediates were detected in the matrices. Similarly, Teles and Maier have also shown that photolyzing carbonazidic acid methyl ester in matrices yields mainly methoxy isocyanate and a small amount of diazenedicarboxylic acid dimethyl ester, formaldehyde and isocyanic acid [11].

Triplet carboalkoxy nitrene can be formed by intramolecular triplet sensitization, which bypasses the singlet carboalkoxy nitrene [3]. For example, sensitized photolysis of carbonazidic acid

* Corresponding author at: Department of Chemistry, University of Cincinnati, PO Box 210172, Cincinnati, OH 45221-0172, USA. Tel.: +1 513 556 3380.
*E-mail address:* annag@uc.edu (A.D. Gudmundsdottir).

1010-6030/$ – see front matter © 2008 Elsevier B.V. All rights reserved.
doi:10.1016/j.jphotochem.2008.10.015

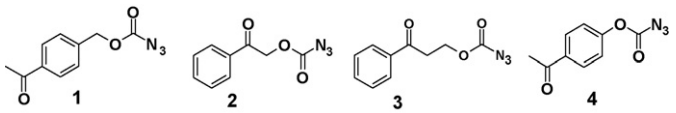

**Scheme 1.**

ethyl ester presumably forms triplet carboethoxy nitrene, which decays by abstracting H-atom from the solvent to form carbamic acid ethyl ester. Furthermore, at cryogenic temperatures Schuster and coworkers irradiated 4-acetylphenoxy carbonyl azide, **4**, which has a built-in triplet sensitizer, and obtained EPR spectrum of the triplet 4-acetylphenoxy carbonyl nitrene intermediate, **4n** [12].

In this article we studied the photoreactivity of azides **1**, **2**, **3**, and **4** that have a build-in triplet sensitizer, to determine the triplet reactivity of these azides in solutions and cryogenic matrices (Scheme 1). The laser flash photolysis of **1**, **2**, **3** and **4** in solutions reveals as expected, that the azides undergo intramolecular energy transfer to from the corresponding triplet nitrenes **1n**, **2n**, **3n** and **4n**, respectively, which mainly decay to form carbamates. In contrast, photolysis of **1**–**3** in argon matrices yields isocyanic acid whereas **4** forms isocyanate derivative. We used IR and UV spectroscopy, and calculations to support the theory that isocyanic acid and isocyanate are formed via secondary photolysis of triplet nitrenes **1n**–**4n** in matrices.

## 2. Experimental

### 2.1. Calculations

All calculations were performed using Gaussian 03 [13]. All geometries were optimized by using the B3LYP level of theory and the 6–31G(d) basis set [14]. Transition states were calculated with the same level of theory and basis set and intrinsic reaction coordinate (IRC) calculations were done to connect the transition states to their reagent and products [17]. The UV spectra were calculated using time-dependent density functional theory (TD-DFT) [15] using B3LYP/6–31G(d) as well. We used self-consistent reaction field (SCRF) method with the integral equation formalism polarizable continuum model (IEFPCM) for solvation calculations [16].

### 2.2. Phosphorescence

The phosphorescence spectra were obtained on a phosphorimeter in frozen ethanol matrices at 77 K.

### 2.3. Laser flash photolysis

Laser flash photolysis were done with excimer lasers (308 nm, 17 ns), which have been described in detailed [18,19]. All spectra and kinetic traces were obtained at ambient temperature. A stock solution of **1**–**4** in were prepared with spectroscopic grade solvents, such that the solutions had an absorption between 0.6 and 0.8 at 308 nm. Typical ~1 mL of the stock solution was placed in a quartz cuvette, which was purged with nitrogen or argon for 5 min. The rates were obtained by fitting an average of 3 kinetic traces. The absorption spectra were measured using an excimer laser in conjunction with an optical multichannel analyzer, or by measuring the absorption point by point over a range of wavelengths.

### 2.4. Matrix isolations

Matrix isolation studies were done using conventional equipment using IR and absorption spectrometers [20,21].

### 2.5. Preparation of starting materials

#### 2.5.1. 4-Acetylbenzyl azidocarbonate (*1*)

A solution of 1-(4-hydroxymethyl-phenyl)-ethanone (2.5 g, 17 mmol) and N,N-dimethyl-aniline (2.02 g, 17 mmol) in dry THF (25 mL) was added slowly to a stirred solution of bis(trichloromethyl) carbonate (1.83 g, 6 mmol) in dry THF (25 mL) while the reaction mixture was maintained at 0 °C. The resulting mixture was stirred at 0 °C for 10 min and then at room temperature for 3 h. The reaction mixture was extracted with diethyl ether (100 mL), the organic layer dried on anhydrous magnesium sulfate and evaporated under vacuum. The resulting 4-acetylbenzyl chloridocarbonate (2.83 g, 15 mmol, 90% yield) was added slowly at room temperature to a vigorously stirred solution of sodium azide (4.23 g, 65 mmol) in dry acetone (50 mL). This mixture was stirred vigorously at room temperature for 4 h. The reaction mixture was concentrated under vacuum, the residue extracted with diethyl ether (150 mL) and the organic layer dried on anhydrous magnesium sulfate and evaporated under vacuum. The residue was purified by a silica gel column eluted with 5% ethyl acetate in hexane to yield 4-acetylbenzyl azidocarbonate (2.33 g, 11 mmol, 65% yield).

IR ($CHCl_3$): 2168, 2143, 1730, 1686, 1235 $cm^{-1}$. $^1H$ NMR (250 MHz, $CDCl_3$): $\delta$ 2.61 (s, 3H), 5.27 (s, 2H), 7.46 (d, 8 Hz, 2H), 7.96 (d, 8 Hz, 2H) ppm. $^{13}C$ NMR (400 MHz, $CDCl_3$): $\delta$ 197.5, 157.5, 139.4, 137.3, 128.7, 128.2, 127.7, 127.2, 69.1, 26.7 ppm. UV–vis (methanol) $\lambda_{max}$: 206, 246, 287 nm. HRMS calculated for $C_{10}H_{11}N_3O_3$ (M+H): 220.0722. Found: 220.0828.

#### 2.5.2. 2-Oxo-2-phenylethyl azidocarbonate (*2*)

A solution of 2-hydroxy-1-phenyl-ethanone (2.3 g, 15 mmol) and N,N-dimethyl-aniline (2.22 g, 15 mmol) in dry THF (25 mL) was added slowly to a stirred solution of bis(trichloromethyl) carbonate (2.02 g, 7 mmol) in dry THF (25 mL) maintained at 0 °C. The resulting mixture was stirred at 0 °C for 10 min and then at room temperature for 3 h. The reaction mixture was extracted with diethyl ether (100 mL), the organic layer dried on anhydrous magnesium sulfate and evaporated under vacuum to yield 2-oxo-2-phenylethyl chloridocarbonate (2.5 g, 13 mmol, 86% yield), which was added slowly at room temperature to a vigorously stirred solution of sodium azide (4.92 g, 75 mmol) in dry acetone (50 mL). The resulting mixture was stirred vigorously at room temperature for 4 h. This mixture was concentrated under vacuum, the residue extracted with diethyl ether (100 mL) and the organic layer dried on anhydrous magnesium sulfate and evaporated under vacuum. The residue was purified by silica gel column eluted with 5% ethyl acetate in hexane to yield 2-oxo-2-phenylethyl azidocarbonate (1.33 g, 6.1 mmol, 41% yield).

IR ($CHCl_3$): 2161, 2128, 1738, 1702, 1256 $cm^{-1}$. $^1H$ NMR (250 MHz, $CDCl_3$): $\delta$ 5.43 (s, 2H), 7.50 (d, 7.5 Hz, 2H), 7.63 (d, 7.5 Hz, 1H), 7.90 (d, 8.0 Hz, 2H) ppm. $^{13}C$ NMR (400 MHz, $CDCl_3$): $\delta$ 198.0, 158.0, 134.2, 133.9, 128.9, 127.8, 66.6 ppm. UV–vis (methanol) $\lambda_{max}$: 206, 246, 287 nm. HRMS calculated for $C_9H_7N_3O_3Na$ (M+Na): 228.0385. Found: 228.0445.

#### 2.5.3. 3-Oxo-3-phenylpropyl azidocarbonate (*3*)

A solution of 3-hydroxy-1-phenyl-propan-1-one (1.8 g, 11 mmol) and dimethylaniline (2.0 g, 11 mmol) in dry THF (25 mL) was added slowly to a stirred solution of bis(trichloromethyl) carbonate (1.32 g, 4.4 mmol) and dry THF (25 mL) maintained at 0 °C. The resulting mixture was stirred at 0 °C for 10 min and then at room temperature for 3 h. The reaction mixture was extracted with diethyl ether (100 mL), the organic layer dried on anhydrous magnesium sulfate and evaporated under vacuum to yield 3-oxo-3-phenylpropyl chloridocarbonate (2.0 g, 10 mmol, 91% yield),

which was added slowly at room temperature to a vigorously stirred solution of sodium azide (3.21 g, 50 mmol) in dry acetone (50 mL). The mixture was stirred vigorously at room temperature for 4 h. The reaction mixture was concentrated under vacuum, the residue extracted with diethyl ether, and the organic layer dried on anhydrous magnesium sulfate and evaporated under vacuum. The residue was purified by silica gel column eluted with 5% ethyl acetate in hexane to yield 3-oxo-3-phenylpropyl azidocarbonate (1.74 g, 8 mmol, 73% yield).

IR ($CHCl_3$): 2199, 2147, 1721, 1683, 1273 $cm^{-1}$. $^1H$ NMR (250 MHz, $CDCl_3$): $\delta$ 3.38 (t, 7 Hz, 2H), 4.67 (t, 7 Hz, 2H), 7.48 (7, 7.5 Hz, 2H), 7.60 (t, 7.5 Hz, 1H), 7.95 (d, 7.5 Hz, 2H) ppm. $^{13}C$ NMR (400 MHz, $CDCl_3$): $\delta$ 196.1, 157.5, 136.3, 133.6, 128.8, 128.1, 63.6, 37.0 ppm. HRMS calculated for $C_9H_7N_3O_3Na$ (M+Na): 242.0542. Found: 242.0580.

### 2.6. Photolysis

Alcohols **9**–**12** and carbamate **11** were identified by HPLC and a GC-MS comparison with independent samples.

#### 2.6.1. Photolysis of *1*

A degassed solution of **1** (300 mg, 1.37 mmol) in dry methanol (100 mL) was irradiated with a medium-pressure arc lamp through a Pyrex filter for 2 h. HPLC analysis of the reaction mixture showed some remaining **1** (15%) and the formation of a major product **3** (71%) and a minor product 1-(4-hydroxymethyl-phenyl)-ethanone (9%). The solvent was removed under vacuum and the resulting oil purified on a neutral alumina column eluted with 20% ethyl acetate in hexane to obtain **1** (45 mg, 0.21 mmol, 15% recovery) and carbamic acid 4-actyl benzyl ester (**5**) as a white solid (159 mg, 0.82 mmol, 60% yield).

M.p.: 88–90 °C. IR ($CHCl_3$): 3408, 3332, 1694, 1673 $cm^{-1}$. $^1H$ NMR (250 MHz, $CDCl_3$): $\delta$ 2.61 (s, 3H), 4.78 (br s, 2H), 5.17 (s, 2H), 7.45 (d, 7.8 Hz, 2H), 7.96 (d, 8.3 Hz, 2H) ppm. $^{13}C$ NMR (400 MHz, $CDCl_3$): $\delta$ 197.7, 156.4, 141.6, 128.6, 127.9, 127.7, 126.6, 66.0, 26.6 ppm. MS (70 eV) m/e 193 ($M^+$), 178, 150, 135, 107, 89, 77. HRMS calculated for $C_{10}H_{13}NO_3$ (M+H): 194.0817. Found: 194.0858.

#### 2.6.2. Photolysis of *2*

A degassed solution of **2** (100 mg, 0.46 mmol) in dry methanol (100 mL) was irradiated with a medium-pressure arc lamp through a Pyrex filter for 1 h. HPLC analysis of the reaction mixture showed some remaining 2 (28%) and the formation of major products 6 (35%) and hydroxy-1-phenyl-ethanone (33%). The solvent was removed under vacuum and the resulting oil purified on neutral alumina column eluted with 20% ethyl acetate in hexane to obtain 2 (28 mg, 0.13 mmol, 28% recovery) and carbamic acid 2-oxo-2-phenyl-ethyl ester (**6**) as a white solid (33 mg, 0.17 mmol 37% yield).

M.p.: 148–150 °C (Ref. [22] 150–152 °C). IR ($CHCl_3$): 3412, 3328, 1695, 1674 $cm^{-1}$. $^1H$ NMR (250 MHz, $CDCl_3$): $\delta$ 5.0 (br s, 2H), 5.35 (s, 2H), 7.47 (d, 7.8 Hz, 1H), 7.63 (t, 7.8 Hz, 2H), 7.93 (d, 8.3 Hz, 2H) ppm. $^{13}C$ NMR (400 MHz, $CDCl_3$): $\delta$ 193.0, 156.0, 134.2, 133.9, 128.9, 127.8, 66.6 ppm.

#### 2.6.3. Photolysis of *3*

A degassed solution of **3** (100 mg, 0.43 mmol) in dry methanol (40 mL) was irradiated with a medium-pressure arc lamp through a Pyrex filter for 14 h. HPLC analysis of the reaction mixture showed some remaining 3 (7%) and the formation of a major product 7 (80%) and smaller amount of 3-hydroxy-1-phenyl-propan-1-one (11%). The solvent was removed under vacuum and the resulting oil purified on HPLC eluted with ethyl acetate and hexane to obtain recovered 3 (19 mg, 0.082 mmol, 19% recovery) and carbamic acid 3-oxo-3-phenyl-propyl ester 7 as a white solid (52 mg, 0.25 mmol, 58% yield).

M.p.: 135–138 °C (Ref. [23] 148–149 °C). IR ($CHCl_3$): 3426, 3332, 1682 $cm^{-1}$. $^1H$ NMR (250 MHz, $CDCl_3$): $\delta$ 3.33 (t, 7 Hz, 2H), 4.53 (t, 7 Hz, 2H), 4.61 (br s, 2H), 7.48 (t, 7.5 Hz, 2H), 7.60 (t, 7.5 Hz, 1H), 7.97 (d, 7.5 Hz, 2H) ppm. $^{13}C$ NMR (400 MHz, $CDCl_3$): $\delta$ 197.2, 156.6, 136.6, 133.4, 128.7, 128.5, 128.1, 128.3, 60.4, 37.8 ppm.

## 3. Results and discussion

### 3.1. Phosphorescence spectra

We measured the phosphorescence spectra of **1**–**3** at 77 K. No significant phosphorescence emission was observed for **1** and **2**, presumably because the triplet ketones are efficiently quenched by intramolecular energy transfer to the azido chromophores. The acetophenone chromophore in **1**–**4** absorbs above 300 nm, whereas the carbonazidic acid ester group absorbs mainly around 280 nm [3]. Thus, by irradiating with light above 300 nm, only the acetophenone chromophore absorbs and forms the triplet state of the ketone [24]. The triplet ketone can transfer its energy to the azido group, which should fall apart to give a triplet carboalkoxy nitrene intermediate (Scheme 1). We can estimate the energy of the triplet-excited ketone in **3** and the analogous acid chloride, **3Cl**, to be around 73 kcal/mol, which is similar to the energy of the lowest triplet ketone in acetophenone (see Fig. 1) [25]. The yield of phosphorescence for **3** is lower than for **3Cl**, presumably since the triplet ketone in **3** decays both by energy transfer to the azido moiety and phosphorescence. However, azide **3** showed the largest amount of phosphorescence of azides **1**–**3**, presumably because it is the most flexible of the azides in this study and thus can be frozen into conformers for which energy transfer is not efficient.

### 3.2. Product studies

Photolysis of **1**–**4** in methanol via a Pyrex filter yielded carbamates **5**–**8** as the major products, and lesser amounts of alcohols **9**–**12**, respectively (Scheme 2). Alcohols **9**, **10**, **11** and **12** are mainly formed by hydrolysis of the corresponding carbamates, and become more prominent when the reaction mixture is heated to remove the solvent. Thus, the product ratios from solution photolysis of **1**–**4** were analyzed directly with HPLC and the conversion kept below 30%. Carbamates **5**, **6** and **7** were also isolated from the product mixture by column chromatography to characterize them.

Carbamates **5**–**8** must come from nitrenes **1n**–**4n**, respectively, abstracting H-atoms from the solvent. This is in agreement with Lwowski et al., who showed that the intermolecular triplet-sensitized photolysis of carbonazidic acid ethyl ester with acetophenone yields carbamic acid ethyl ester [3]. Similarly, Schuster and coworkers showed that photolyzing **4** in the presence of

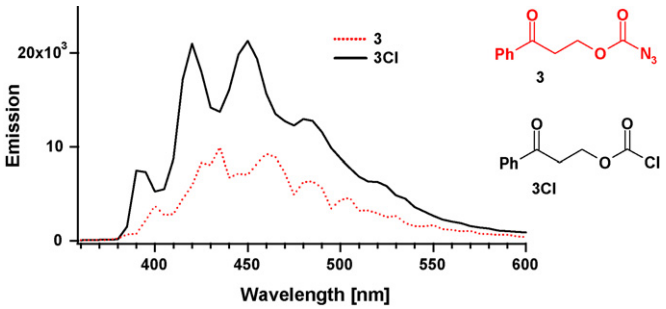


**Fig. 1.** Phosphorescence of 3 and 3Cl.

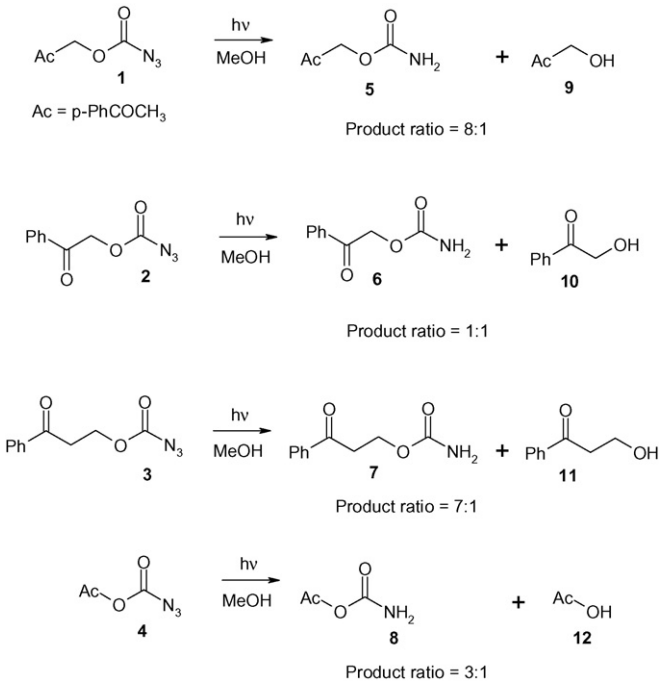


**Scheme 2.**

alkenes yields non-stereospecific aziridine products, as expected for trapping nitrene **4n** with alkenes [12]. However, irradiating **4** in tert-butyl alcohol gives **8**, **12**, **13** and **14** (Scheme 3). Schuster et al. concluded that **13** is formed from the insertion of the singlet nitrene **4s** into the solvent and **14** comes from **4s** inserting into its phenyl ring. Thus, Schuster et al. suggest that the triplet and the singlet nitrene are in equilibrium with each other in the viscous tert-butanol, which is reasonable since the energy gap between the singlet and the triplet nitrene has been estimated to be between 3 and 8 kcal/mol [6–9]. In comparison, Schuster et al. showed that photolysis of **4** in a less viscous solvent, cyclohexane yields mainly products attributed to triplet nitrene **4n**.

Similarly, we did not observe any photoproducts from **1**–**4** in methanol which can be attributed to trapping the corresponding singlet carboalkoxy nitrenes and thus it is unlikely that singlet and triplet nitrenes are in equilibrium, because the triplet nitrenes react faster in methanol that is a good H-atom donor than in tert-butanol.

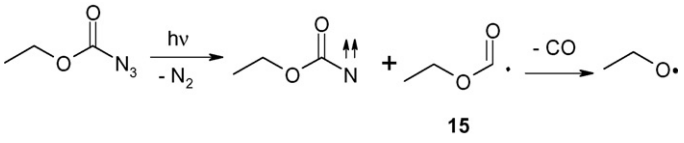


**Scheme 4.**

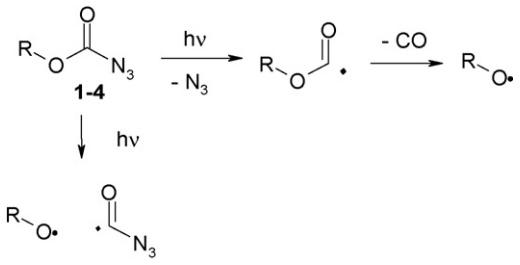


**Scheme 5.**

Buron and Platz have shown that direct photolysis of carbonazidic acid ethyl ester yields triplet nitrene and radical **15** (Scheme 4) [6], which comes from cleavage of the C–N ester azide bond. Radical **15** decays by expelling carbon monoxide and forming an ethoxy radical. It is possible that **1**–**4** undergo similar photocleavage which will results in formation of **9**–**12** (Scheme 5). It can also be theorized that **9**–**12** come from **1**–**4** undergoing cleavage of the C–O bonds as shown in Scheme 5.

Thus, photolysis of **1**–**4** in methanol supports that the main reactivity of **1**–**4** is forming triplet nitrenes, which decay by H-atom abstraction to form carbamates **5**–**8**.

### 3.3. Calculations

We used molecular modeling to aid the characterization of the intermediates formed upon irradiation of **1**–**4** and to access the feasibility of various reaction for the triplet state of these azides and the corresponding triplet nitrenes. The calculations demonstrated that **1**–**4** each have several minimal-energy conformers that are within a few kcal/mol of each other. The structures of the corresponding triplet nitrenes **1n**–**4n** and isocyanates **1i**–**4i** were also optimized, and the IR spectra of all species were calculated (Scheme 6).

We used azide **16** as a model for **1**–**4**, and calculated the most feasible reactions on its triplet surface. Azide **16** is an excellent model for **1**–**4**, because the most significant difference between **16** and

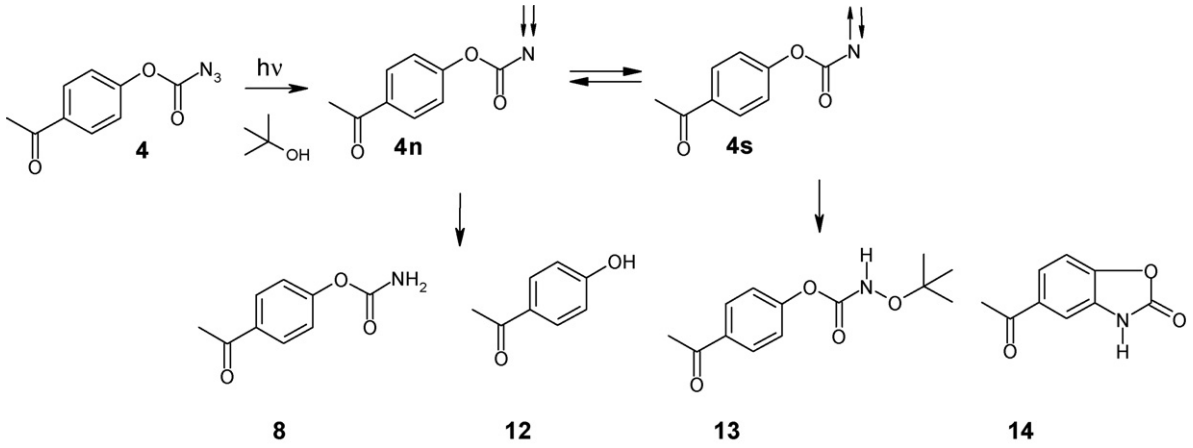


**Scheme 3.**

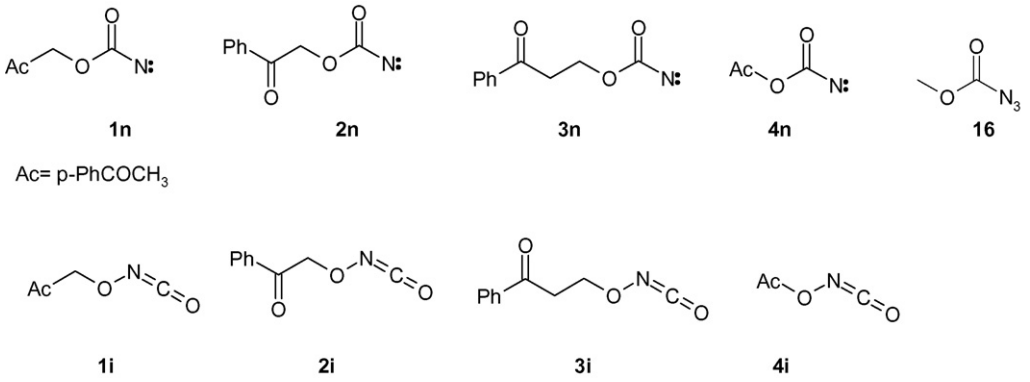


**Scheme 6.**

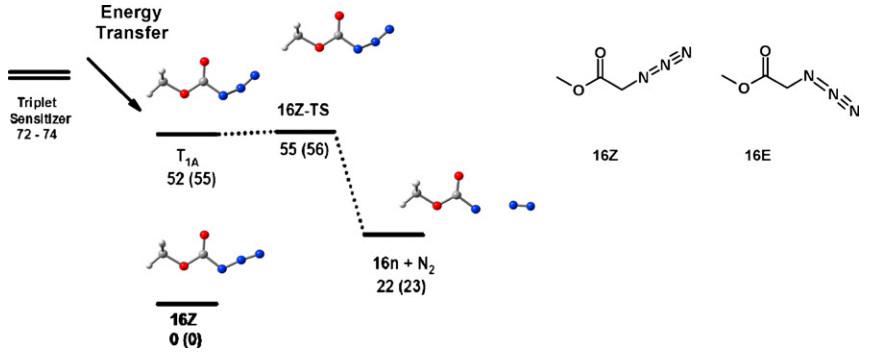


**Fig. 2.** Points on the potential energy surfaces (kcal/mol) for triplet reactivity of **16Z** in the gas phase and in methanol (parenthesis). $T_{1A}$ is the optimized triplet state of **16Z**. 16Z-TS is the calculated transition state for forming **16n** and a nitrogen molecule.

**1**–**4** is the acetophenone moiety that serves only as the triplet sensitizer. We optimized the Z and E conformers of **16** and found that the Z conformer of **16** is about 1 kcal/mol lower in energy than its E conformer. This is similar to the result obtained by Liu et al. [9] We optimized the first excited triplet state ($T_{1A}$) of **16**, where an electron has been promoted from a filled orbital on the azide moiety into the $\pi^*$ orbital of the azide and found it was located 52 and 55 kcal/mol above the ground state ($S_0$) of **16**, in the gas phase and in methanol, respectively. In $T_{1A}$ of **16Z** the N-N-N is bend 120° and the N1–N2 bond length is 1.47 Å. The C=O and the C–O bond lengths are 1.21 and 1.33 Å, respectively in $T_{1A}$ of **16Z** and thus similar to the C=O and C–O bond lengths in $S_0$ of **16Z**.

We calculated the triplet transition state for cleaving **16Z** to form a nitrogen molecule and triplet nitrene **16n** (see Fig. 2). This transition state was only 3 kcal/mol above the $T_{1A}$ of **16Z** in the gas phase and 1 kcal/mol in methanol. Intrinsic reaction coordinate (IRC) [31] calculations allowed us to correlate $T_{1A}$ in **16Z** and **16n** to this transition state. Since the energy of $T_{1A}$ in **16** is well below the energy of the triplet sensitizer in **1**–**4** and the transition state for forming **16n** from $T_{1A}$ of **16** is located within a few kcal/mol, the calculations support that triplet-sensitized photolysis of **1**–**4** can produce **1n**–**4n**, respectively. The effect of solvation of the reactivity of **16** was calculated using IEFPCM model with methanol and acetonitrile [16]. The effect of solvation was not significant for either methanol or acetonitrile.

In comparison, the triplet transition states for **16Z** to fall apart to give an azido and methoxycarbonyl radical is 97 kcal/mol above $S_0$ of **16Z**, and the triplet transition state for **16Z** to form a methoxy and acyl azide radical is located 104 kcal/mol above $S_0$. The calculations indicate that cleavage of either the C–N or the C–O bonds in **16** must come from an excited state that is higher in energy than $T_{1A}$ of **16**. Similar calculations for **16E** give comparable results. Since the energy of the triplet sensitizers in **1**–**4** is between 72 and 74 kcal/mol [25] above their $S_0$ and the energy of the triplet transition states for the C–O and C–N bond cleavages are considerable higher, it is highly unlikely that triplet sensitization will result in the cleavage of the C–O or the C–N bond in **1**–**4**.

We calculated the transition state for **16n** to form methoxy (**17**) and cyanato (**18**) radicals, which are located ~34 kcal/mol above **16n** (Fig. 3). IRC calculations correlate this transition state to **16n** and the methoxy and cyanato radicals. Since this transition state is ~34 kcal/mol above **16n** this process can only be expected to take place photochemically. We optimized the structure of the possible products from the methoxy and cyanato radicals and found that methoxy isocyanate, and formaldehyde and isocyanic acid, are 15 and 45 kcal/mol more stable than **16n**, respectively. Thus, it is possible that photolysis of **1n**–**4n** results in formation of alkoxy and cyanato radicals, which can either, recombine to isocyanate **1i**–**4i**

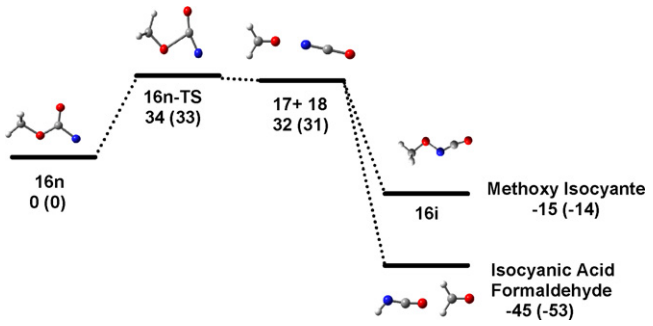


**Fig. 3.** Points on the potential energy surfaces (kcal/mol) for triplet reactivity of **16n** in the gas phase and in methanol (parenthesis). 16n-TS is the calculated transition state for **16n** to fall apart to yield **17** and **18**.

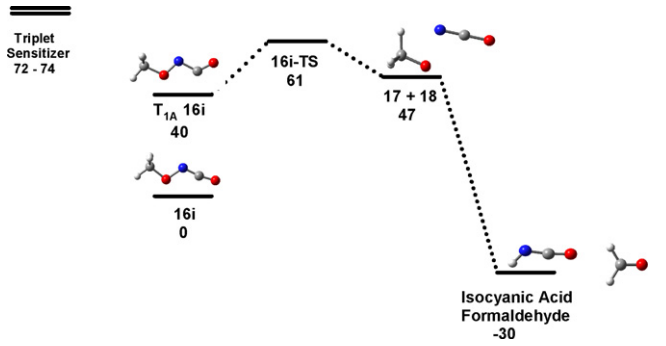


**Fig. 4.** Points on the potential energy surfaces (kcal/mol) for triplet reactivity of **16i** in the gas phase. 16i-TS is the calculated transition state for **T1** of **16i** to fall apart to yield **17** and **18**.

or undergo intermolecular H-atom abstraction to form isocyanic acid and the corresponding aldehyde.

We optimized the first triplet state ($T_1$) of methoxy isocyanate (**16i**), which is located 40 kcal/mol above $S_0$ of **16i** (Fig. 4). The C–N bond lengthens from 1.23 Å in $S_0$ to 1.40 Å in $T_1$ of **16i** and the N=C=O angle goes from 170 to 123°. The lengthening of the C=N bond in $T_1$ in **16i** is reflected by the calculated IR stretch of N=C=O chromophore, which is at 1819 $cm^{-1}$, in comparison, the calculated IR band for the N=C=O moiety in $S_0$ of **16i** is at 2293 $cm^{-1}$. We calculated the transition state for $T_1$ of **16i** to fall apart to form methoxy and cyanato radicals and found it was located 21 kcal/mol above $T_1$. Thus, sensitized photolysis of isocyanates **1i**–**4i** can form vibrationally hot triplet states of **1i**–**4i** that can cleave to form alkoxy and cyanato radicals.

Finally, we used time-dependent density functional theory (TD-DFT) [15] to estimate the absorption spectra for **1n**–**4n** (Table 1). The effect of solvation was calculated using IEFPCM model with methanol and acetonitrile [16].

### 3.4. Laser flash photolysis

The transient spectrum obtained by laser flash photolysis (17 ns, 308 nm) of **1** in acetonitrile, immediately after the laser pulse over a 20 ns window, has $\lambda_{max}$ at 330 nm (Fig. 5), which we assign to the triplet ketone in **1**. This assignment is further supported by laser flash photolysis of **9** that yields a similar transient of its triplet ketone. In comparison, the transient spectrum obtained 1000 ns after the laser pulse showed an absorbance band with a maximum absorbance at around 340 nm. We assign the band at 340 nm to **1n**. Laser flash photolysis of **1** in methanol, ethanol and dichloromethane resulted in similar transient spectra as obtained in acetonitrile. Buron and Platz reported that triplet carboethoxy nitrene in Freon solution has a broad, transient spectrum with $\lambda_{max}$

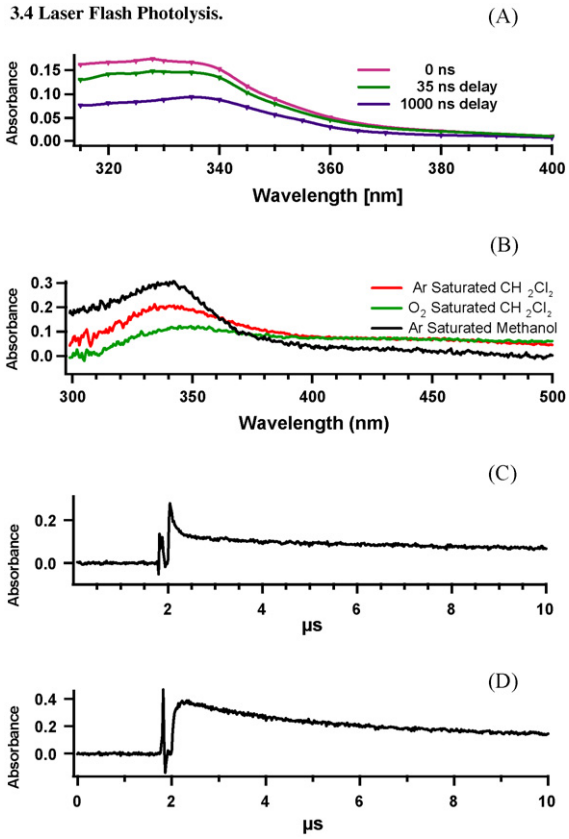


**Fig. 5.** Transient spectra from laser flash photolysis of **1** (A) In acetonitrile at different time delays. (B) In methanol and dichloromethane immediately after the laser pulse over a 500 ns window. (C) Kinetic trace at 306 nm in acetonitrile. (D) Kinetic trace at 344 nm in acetonitrile.

**Table 1**
Major absorption spectral features (nm, (oscillator strength)) for **1n**, **2n**, **3n** and **4n**[a,b].

| | Major electronic transition above 300 nm | | | | | | |
|---|---|---|---|---|---|---|---|
| **1n** | | | | | | | |
| GP[c] | 313 (0.0036) | 332 (0.0061) | 367 (0.0144) | 411 (0.0132) | 617 (0.0095) | | |
| $CH_3CN$ | 311 (0.0038) | 353 (0.0045) | 372 (0.0017) | 391 (0.0286) | 429 (0.0022) | 519 (0.0031) | 673 (0.0009) |
| MeOH | 311 (0.0037) | 353 (0.0045) | 372 (0.0017) | 391 (0.0284) | 428 (0.0022) | 519 (0.0031) | 617 (0.0009) |
| **2n** | | | | | | | |
| GP | 309 (0.0043) | 346 (0.0067) | 359 (0.0011) | 396 (0.0036) | 520 (0.0117) | | |
| $CH_3CN$ | 309 (0.0036) | 359 (0.0078) | 393 (0.0017) | 405 (0.0047) | 584 (0.0148) | 636 (0.0023)) | |
| MeOH | 309 (0.0036) | 359 (0.0078) | 393 (0.0016) | 406 (0.0047) | 584 (0.0148) | 636 (0.0022) | |
| **3n** | | | | | | | |
| GP | 313 (0.0040) | 363 (0.0102) | 411 (0.0091) | 500 (0.0011) | | | |
| $CH_3CN$ | 313 (0.0036) | 370 (0.0008) | 371 (0.0014) | 376 (0.0069) | 381 (0.0010) | 421 (0.0152) | 582 (0.0014) |
| MeOH | 313 (0.0036) | 370 (0.0009) | 371 (0.0012) | 376 (0.0070) | 380 (0.0010) | 420 (0.0151) | 581 (0.0014) |
| **4n** | | | | | | | |
| GP | 309 (0.0074) | 314 (0.0035) | 365 (0.0048) | 383 (0.0018) | 394 (0.0021) | 519 (0.0031) | 642 (0.0657) |
| $CH_3CN$ | 312 (0.0031) | 315 (0.0102) | 365 (0.0062) | 394 (0.0025) | 582 (0.0012) | 694 (0.0862) | |
| MeOH | 312 (0.0031) | 315 (0.0101) | 365 (0.0062) | 394 (0.0024) | 581 (0.0012) | 694 (0.0856) | |

[a] The wavelength of the electronic transitions in nm.
[b] Number in parenthesis is the calculated oscillator strength (*f*) for the electronic transition.
[c] GP: gas phase.

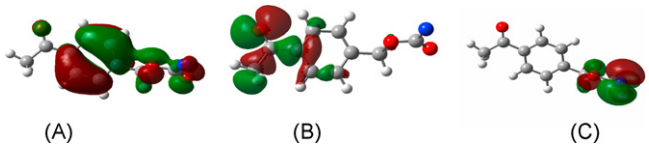


**Fig. 6.** The most intense absorption band in **1n** is mainly due to electron transition from the π-orbital (A) and the lone pair in the ketone (B) to one of the singly occupied orbitals on the nitrogen (C).

~400 nm [6]. TD-DFT calculation for carboethoxy nitrene, locate the most intense electronic transitions at 412 nm ($f$ = 0.0090) and 364 nm ($f$ = 0.0082), which are due to promotion of an electron from the lone pairs on the oxygen atoms to one of the singly occupied orbitals on the nitrogen atom [6]. The calculated UV spectrum for **1n** has the most intense transition at 367 nm in the gas phase, which is predominantly an electronic transition from the π orbitals of the aromatic system to one of the singly occupied orbitals on the nitrogen atom (Fig. 6). TD-DFT calculation in methanol and acetonitrile put the most intense band at ~390 nm and it is due to a mixed electronic transition out of the π-orbitals and the lone pair on the ketone oxygen atom into the half full orbital on the nitrogen atom (Fig. 6). Hence, the absorption for **1n** was expected to shift to a lower wavelength in comparison to carboethoxy nitrene. The absorption of **1n** was not quenched in oxygen-saturated solution, but the yield was decreased, because some of the triplet ketone in **1** is quenched. We determined the lifetimes of the triplet ketone in **1** and **1n** from the bi-exponential decay of the transient at 344 nm to be 100 ns and 2 μs, respectively, in methanol. Furthermore, we were able to measure that the rate of formation of **1n** at 306 nm to be the same as the decay of the triplet ketone or ~$1.0 \times 10^7$ $s^{-1}$. In comparison, the triplet ketone in **9** is longer lived, 0.7 μs in acetonitrile, because it does not decay by intramolecular energy transfer.

Laser flash photolysis of **2** in acetonitrile, methanol and ethanol yielded absorption due to **2n** ($\lambda_{max}$ ~ 350 nm and a much weaker band at ~450 nm), and its triplet ketone ($\lambda_{max}$ ~ 320 nm, Fig. 7). The latter can be assigned to the triplet ketone based on its similarity to the transient spectrum of acetophenone [26]. The absorption of **2n** fits reasonably with its calculated spectra (Table 1), which show major bands at 359 and 584 nm in both methanol and acetonitrile. The calculated band at 359 nm fits well with the observed $\lambda_{max}$ ~ 350 nm but we did not observe an intense band above 500 nm, only a weak band ~450 nm. However, the assignment of the transient with $\lambda_{max}$ ~ 350 nm to **2n** was further supported by

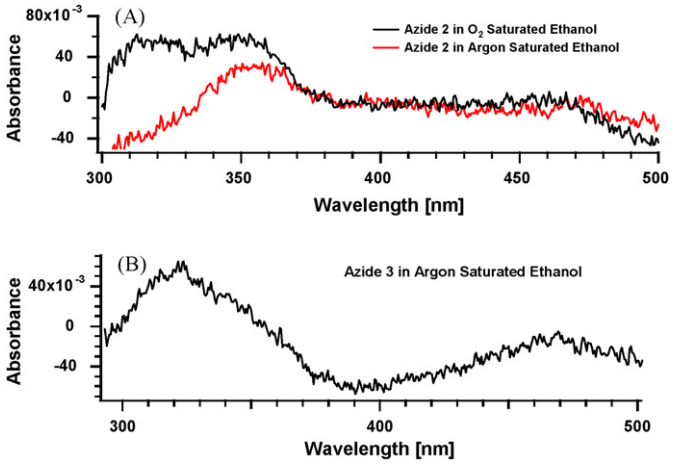


**Fig. 7.** Transient spectra obtained by laser flash photolysis of (A) **2** and (B) **3** in ethanol. The spectra were recorded immediately after the laser pulse over a window of 500 ns.

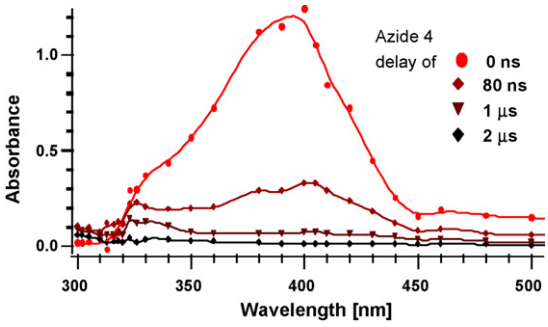


**Fig. 8.** Transient spectra obtained by laser flash photolysis of **4** in nitrogen-saturated methanol.

obtaining a transient spectrum in oxygen-saturated ethanol. The oxygen quenches the triplet ketone in **2** ($\lambda_{max}$ ~ 320 nm) and thus decreases the yields of the **2n** (Fig. 8). The decay of the transient at 350 nm in argon- or nitrogen-saturated solutions is best fitted as bi-exponential decay. The shorter lived component is due to the triplet ketone that decays with a rate of $3.3 \times 10^6$ $s^{-1}$, whereas the longer lived component (**2n**) has a lifetime of ~2 μs.

Similarly, the transient spectra obtained by laser flash photolysis of **3** in acetonitrile and methanol showed a band at 320 nm which we assign to the triplet ketone in **3**, whereas **3n** has a transient absorption with $\lambda_{max}$ at ~350 nm and a broad but less intense band with $\lambda_{max}$ ~ 460 nm (Fig. 7). The most intense calculated electron transitions for **3n** are located at 370 and 420 nm, which support the assignment of this transient to **3n**. In oxygen-saturated solutions both the absorption of the triplet ketone in **3** and **3n** are quenched. The decay of the triplet ketone in **3** is $1.6 \times 10^6$ $s^{-1}$ which is somewhat slower than observed for **2**, because the distance between ester azide and the triplet ketone chromophores is larger. The lifetime of **3n** is ~ 2 μs in methanol.

Laser flash photolysis of **4** showed the transient spectra of the triplet ketone at 400 nm, which decays with a rate of $5 \times 10^6$ $s^{-1}$, whereas the transient due to **4n** has $\lambda_{max}$ ~ 320 nm and has a lifetime of 2 μs in methanol (Fig. 8). The transient spectrum of the triplet ketone is similar to what Schuster and coworkers reported for **4** [12], whereas the assignment of the absorption band with $\lambda_{max}$ ~ 320 nm to **4n** is based on the TD-DFT calculations (Table 1). The major calculated electron transition for **4n** in methanol are located at 315 nm ($f$ = 0.0102) and 694 nm ($f$ = 0.0856). The transition at 315 nm is mainly due to electron being promoted out of π-orbitals to one of the half full p-orbital on the nitrogen atom. However, we cannot measure the transient absorption above 600 nm and verify that **4n** absorbs in that region.

Due to the acetophenone chromophore, the transient spectra of nitrenes **1n**–**4n** are different from the transient spectrum of **16n** and the TD-DFT calculations support this difference. The laser flash photolysis demonstrate that **1n**–**4n** have similar lifetime in methanol since they decay by intramolecular H-atom abstraction to form the corresponding carbamates. Furthermore, the lifetimes of **1n**–**4n** are similar to the reported lifetime of triplet nitrene **16n** in methanol [6]. The rate of the energy transfer in **1**–**4** is affected by the intramolecular distance between the ketone and the ester azide moieties and by the energy of the triplet ketone. The rate of the energy transfer in **3** is the slowest, as expected, whereas it is the fastest in **1**. Schuster and coworkers have previously shown that the triplet ketone chromophore in **4** has a lifetime of 100 ns in tert-butyl alcohol, which is similar to what we observe [12]. The rate of energy transfers in **1**–**4** are slower than we observed in 2-azido-1-phenyl ethanone [30], which is reasonable because of the increased distance between the ketone and the azido chro-

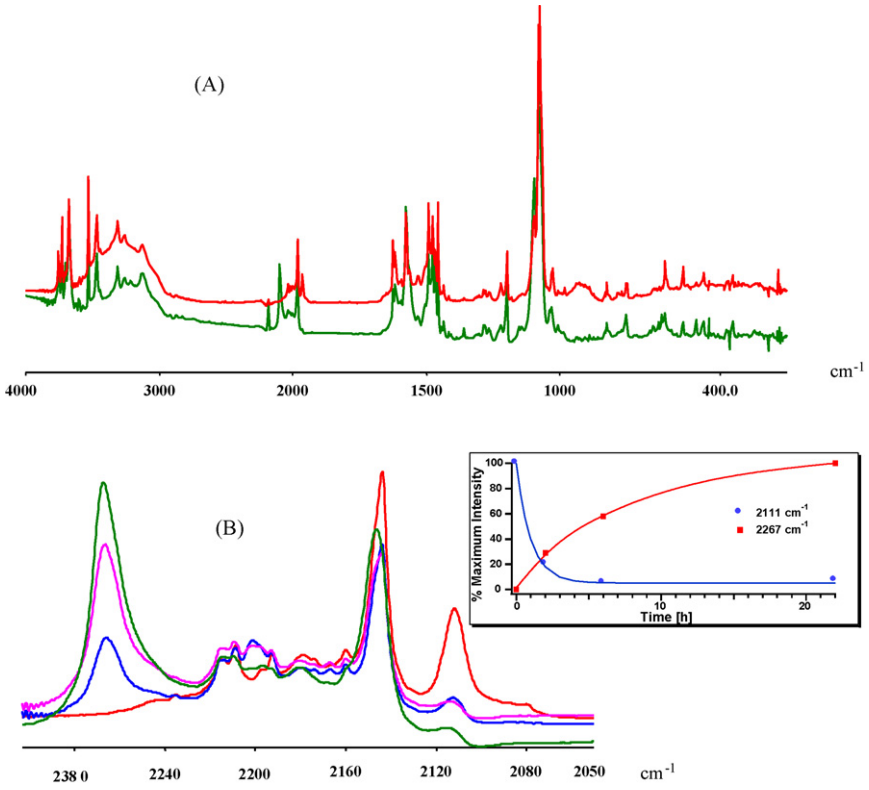


**Fig. 9.** IR spectra of **1** in argon matrices. (A) Before (red) and after 22 h of irradiation (green). (B) The expanded IR spectra between 2300 and 2050 $cm^{-1}$ before (red), after 2 h (blue), 6 h (pink) and 22 h (green) of irradiation. The insert displays the rate of disappearance for the band at 2111 $cm^{-1}$ and the rate of formation for the band at 2267 $cm^{-1}$. (For interpretation of the references to color in this figure legend, the reader is referred to the web version of the article.)

mophores in **1**–**4**. Furthermore, the energy of triplet ester azides is ~55 kcal/mol above their $S_0$ whereas triplet alkyl azides have been estimated to be only ~44 kcal/mol above their $S_0$ [31].

### 3.5. Matrix isolation spectra

We deposited **1**–**4** in argon matrices at 14 K. The vibrational stretch of the azide chromophore was observed between 2100 and 2200 $cm^{-1}$ (see Figs. 9–13). Irradiating azides **1**–**3** in the matrices reduced their intensities. The most significant bands that were formed by irradiation were at ~2267–2247 $cm^{-1}$ and we assign them to isocyanic acid based on comparison with literature [27]. Crowley and Sodeau showed that isocyanic acid has strong absorbance bands at 2267, 2261 and 2259 $cm^{-1}$ in argon matrices [27]. Apart from the reduction of the azide bands and the formation of the isocyanic acid bands, the IR spectra of **1**–**3** before and after photolysis were remarkably similar, presumably because the majority of the IR bands belong to the triplet sensitizer, which is unchanged upon photolysis. We quantified at several different time intervals, how much the azide bands were depleted compared to how much the isocyanic acid bands grew, and found the rates to be different. This is best seen for **1** (see Fig. 9B); after 2 h of irradiation, the azide band at ~2111 $cm^{-1}$ was reduced by 80%; after 6 h, it decreased by 95%; and after 22 h the intensity decreased by 93%. After 2 h of irradiation, the isocyanic acid band at 2267 $cm^{-1}$ had grown in and had an intensity of 0.07; after 6 h its intensity was 0.14 and after 22 h the intensity was 0.24. Thus, the intensity of the isocyanic acid band increased significantly, although we saw very little additional depletion of the azide bands. The azido band at 2143 $cm^{-1}$ did not react significantly upon irradiation and thus it is likely that this band is due to conformer of azide **1**, which is not well aligned for energy transfer and that the triplet ketone decays by phosphorescence rather than undergoing energy transfer. We plotted the intensity of the azido band at 2111 $cm^{-1}$ and isocyanic acid band at 2267 $cm^{-1}$ versus time of irradiation in Fig. 9, which further illustrates that the rate of depletion of the azido band is faster than the rate of formation of the isocyanic band.

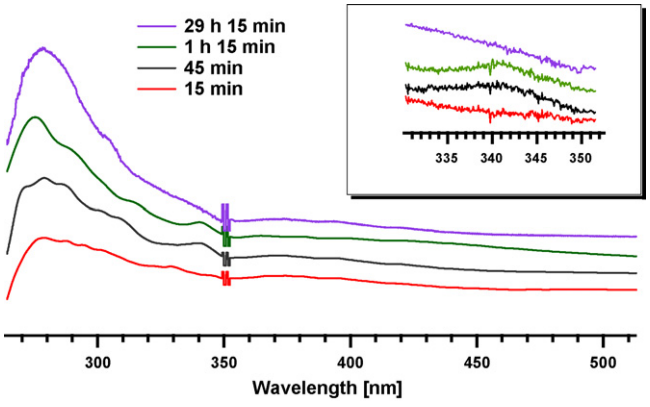


**Fig. 10.** Differential UV spectra of **1** in argon matrices after 1/4 (red), 3/4 (black), 1 (1/4) (green), and 29 (1/4) (purple) h of irradiation.

Since the rates for depleting the azide bands and forming isocyanic acid were the most different for **1**, we used UV absorption spectroscopy also to follow its reactivity in matrices. Irradiation of **1** in argon matrices produced an absorption band with $\lambda_{max}$ at 343 nm, which we assign to **1n**, based on its similarity to the transient spectra of **1n** in solutions (Fig. 10). The band at 343 nm decreased upon further irradiation and, after 3 (1/4) h of irradiation, it was depleted. It should be pointed out that the argon matri-

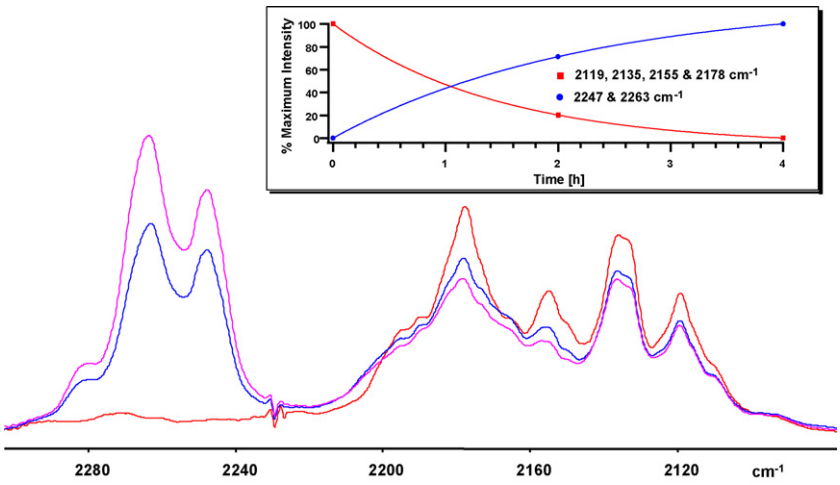


**Fig. 11.** IR spectra of **2** in argon matrices before (red), after 2 h (blue) and 4 h (pink) of irradiation.

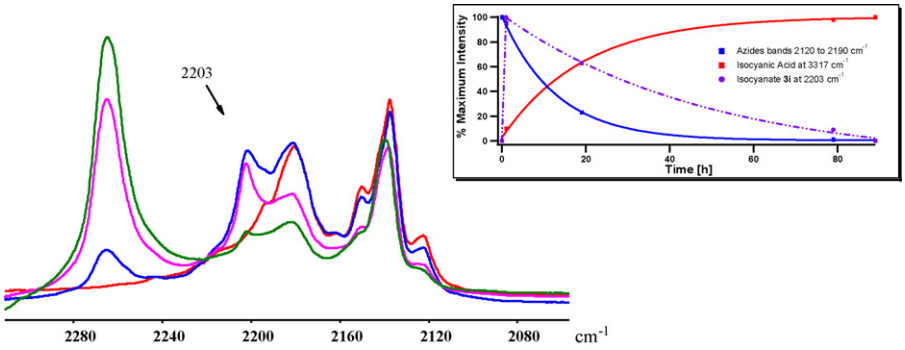


**Fig. 12.** IR spectra of azide 3 in argon matrices before (red) and after 1 h (blue), 19 h (pink) and 79 h (green) of irradiation.

ces prepared for UV absorption experiments are thinner than the matrices analyzed with IR spectroscopy and thus the reaction times faster. Photolyzing **1** also produced a band with $\lambda_{max}$ at ~280 nm, which we assign to acetyl benzaldehyde, because the absorption spectrum for acetyl benzaldehyde is very similar.

Azide **2** has four azide vibrational bands at 2119, 2135, 2155 and 2178 $cm^{-1}$ (Fig. 11). Photolysis reduced the intensities of the azide bands, and the most significant bands that formed were at 2247 and 2263 $cm^{-1}$. We assign both these bands to isocyanic acid. Presumably, two isocyanic acid bands are formed from **2** in different environments within the argon matrices. Typical matrix effects cause splitting of a few wave numbers, which fits with our observations [29]. We also observed the N–H stretch for isocyanic acid at 3313 $cm^{-1}$.

Azide **3** has four azide bands, at 2122, 2140 2150 and 2183 $cm^{-1}$ (Fig. 12). Irradiation reduced the intensity of the bands, and we observed a new band at 2203 $cm^{-1}$ that we assigned to isocyanate **3i**. We base our assignment on the observation of Lwowski et al. that methoxy isocyanate has a strong vibrational band at 2209 $cm^{-1}$ [10]. Furthermore, Maier et al. also reported a strong band at 2204 $cm^{-1}$ for methoxy isocyanate in argon matrices [11]. The vibrational band at 2203 $cm^{-1}$ grew in for the first 19 h of irradiation, but decreased upon further photolysis. During this decrease, we observed the formation of isocyanic acid bands at 3317, 2260 and 771 $cm^{-1}$. The calculated isocyanate band for **3i** is at 2293 $cm^{-1}$, and scaling of 0.96 [28] put this band at 2201 $cm^{-1}$, which is in excellent agreement with the experimental band. Isotope labeling with $^{15}N$ shifted the band at 2203–2190 $cm^{-1}$, which is consistent with the calculated shift of ~10 $cm^{-1}$ for **3i**.

The calculated IR spectrum of **3n** has vibrational bands at 1047, 948 and 639 $cm^{-1}$ that are affected by $^{15}N$ labeling. The calculated intensity of the 1047 $cm^{-1}$ bands is 33 km/mol whereas the

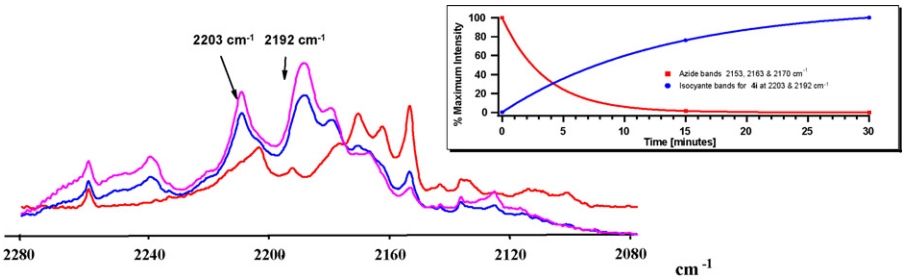


**Fig. 13.** IR spectra of azide 4 in argon matrices before (red) and after 15 min (blue) and 30 min (pink) of irradiation.

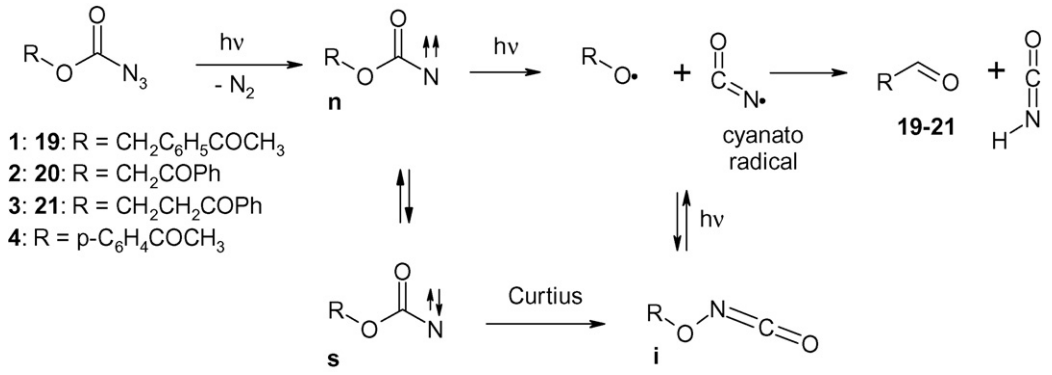


**Scheme 7.**

other two band have intensities of less than 7 km/mol. These bands shifted to 1043, 945 and 629 $cm^{-1}$, respectively, upon $^{15}N$ substitution. Thus, these three bands are the vibrational bands that involve the C–N bond in **3n**. Even with the aid of $^{15}N$ labeling, we were not able to locate these bands, presumably because their intensity is low.

Irradiating **4** in matrices led to the depletion of the azide bands at 2153, 2162 and 2170 $cm^{-1}$ (Fig. 13). The most significant bands that grew in were at 2203 and 2192 $cm^{-1}$, which we assigned to isocyanate **4i** based on its similarity to **3i**. Presumably, two different conformers of **4i** arise from different conformers of **4**, however, we cannot rule out that matrix splitting is responsible for the two isocyanate bands. We also observed the formation of IR bands at 1163, 951, 909, 834, 580 and 517 $cm^{-1}$, which belonged to **4i**. This assignment is supported by calculations that place the isocyanate bands for **4i** at 2296 and 2297 $cm^{-1}$. Scaling with 0.96 locates the calculated isocyanate bands at 2204 and 2205 $cm^{-1}$, which is in excellent agreement with experiment [28].

Finally, we deposited carbonazidic acid ethyl ester, which does not have an intramolecular sensitizer, into argon matrices. Prolonged irradiation of this azide in matrices through a Pyrex filter did not yield any products, whereas irradiation through quartz yielded ethoxy isocyanate and isocyanic acid. This experiment verifies that the reactivity of **1**–**4** in matrices is taking place via triplet sensitization and not direct irradiation. The results of the quartz photolysis of carbonazidic acid ethyl ester in argon matrices is very similar to what Lwowski and coworkers observed for carbonazidic acid methyl ester [10].

Photolyzing **1**–**3** in argon matrices yielded isocyanic acid as the final product, but in a stepwise manner. It is unlikely that azides **1** and **2** formed isocyanic acid via isocyanates **1i** and **2i**, respectively, because we did not observe any IR bands that could be assigned to isocyanates, as for azide **3**. In comparison, prolonged irradiation of isocyanate **3i** yields the more stable isocyanic acid and aldehyde **21** (Scheme 7). Since the azide bands in **1**–**3** were depleted faster than the isocyanic acid bands were formed, we propose that irradiating azide **1**–**3** in matrices yields **1n**–**3n**, respectively, and that the nitrene intermediates absorb another photon to form alkoxy and cyanato radicals. The cyanato radical can then abstract an H-atom from the alkoxy radical to form isocyanic acid and the corresponding aldehyde (**19**–**21**). We cannot account for the aldehyde bands in the matrices with IR spectroscopy, since their carbonyl bands are buried under the carbonyl band of the starting material. Neither, can we observe triplet nitrenes **1n**–**3n** directly in matrices using IR spectroscopy. Nevertheless, the formation of nitrene intermediate in matrices was confirmed by UV absorption spectroscopy.

Likewise, matrix irradiation of **4** yields **4i**, presumably via secondary photolysis of **4n** to form alkoxy and cyanato radicals that recombine, since the aryloxy radical does not have any abstractable H-atom. The formation of **4n** in matrices is in agreement with findings by Schuster and coworkers, who demonstrated that irradiating **4** at 8 K gives rise to an EPR signal that they assigned to **4n** [12]. It is not likely that **1n**–**4n** are in equilibrium with their singlets in matrices at 14 K, since the singlets are at least 3 kcal/mol higher in energy. Furthermore, Liu et al., have calculated that the transition state for singlet carbomethoxy nitrene (**16 s**) to undergo Curtius rearrangement to form methoxy isocyanate is between 9 and 14 kcal/mol above **16 s** and thus not likely to take place from relaxed singlet nitrenes at cryogenic temperature [9].

Thus, triplet ester nitrenes **1n**–**4n** are photolabile in matrices. Similarly, triplet phenyl nitrene and alkyl nitrene have also been reported to undergo secondary photoreaction in matrices [31,32]. Furthermore, we theorize, that direct photolysis of azide **16** in matrices yields singlet nitrene **16 s**, which then intersystem crosses to form triplet nitrene **16n**. The rate of intersystem crossing from the singlet to the triplet has been estimated to be $10^8$ $s^{-1}$ at room temperature [6], and should not be affected strongly by temperature. Thus, singlet **16 s** relaxes to **16n**, which undergoes secondary photolysis to yield methoxy isocyanate, and explains why direct and sensitized photolysis of ester azides in matrices yield similar products. This theory would also explain the formation of diazenedicarboxylic acid dimethyl ester that Teles and Maier [11] observed along with methoxy isocyanate by irradiating carbonazidic acid ethyl ester in matrices, since triplet nitrenes generally dimerize to form azodimers [32]. Furthermore, this is in agreement with Wasserman et al. finding that low temperature photolysis of carbonazidic acid ethyl ester results in EPR signal [5].

## 4. Conclusions

Our results show that photolyzing azides **1**–**4** in methanol results in intramolecular energy transfer to form triplet ester nitrenes **1n**–**4n** that decay mainly by H-atom abstraction from the solvent. Photolyzing **1**–**3** in argon matrices at low temperature yields isocyanic acid from secondary photolysis of **1n**–**3n**. Similarly, photolyzing **4** in matrices yields isocyanate **4i** via secondary photolysis of **4n**. Thus, triplet ester nitrenes can be formed selectively via intramolecular photosensitization, but these intermediates are themselves highly photoreactive.

## Acknowledgments

We thank the National Science Foundation (CHE 0703920) and the Ohio Supercomputer Centre for supporting this work. We also thank Professor M. S. Platz at The Ohio State University and Profes-

sor J. C. Scaiano at the University of Ottawa for allowing us to use some of their instruments. R. S. M. is grateful to the University of Cincinnati Research Council for its support.

## References

[1] M.S. Platz, Nitrenes, in: R.A. Moss, M.S. Platz, M. Jones Jr. (Eds.), Reactive Intermediate Chemistry, John Wiley & Sons, Inc., Hoboken, NJ, 2004, pp. 501–559.
[2] (a) M. Holzinger, J. Abraham, P. Whelan, R. Graupner, L. Ley, F. Hennrich, M. Kappes, A. Hirsch, J. Am. Chem. Soc. 125 (2003) 8566;
(b) M. Holzinger, O. Vostrowsky, A. Hirsch, F. Hennrich, M. Kappes, R. Weiss, F. Jellen, Angew. Chem., Int. Ed. English 40 (2001) 4002.
[3] (a) W.L. Lwowski, F.P. Woerner, J. Am. Chem. Soc. 87 (1965) 5491;
(b) W. Lwowski, T.W. Mattingly Jr., J. Am. Chem. Soc. 87 (1965) 1947.
[4] J.S. McConaghy Jr., W. Lwowski, J. Am. Chem. Soc. 87 (1965) 5490.
[5] E. Wasserman, Prog. Phys. Org. Chem. 8 (1971) 319.
[6] C. Buron, M.S. Platz, Org. Lett. 5 (2003) 3383.
[7] A.P. Scott, M.S. Platz, L. Radom, J. Am. Chem. Soc. 123 (2001) 6069.
[8] E.A. Pritchina, N.P. Gritsan, A. Maltsev, T. Bally, T. Autrey, Y. Liu, Y. Wang, J.P. Toscano, Phys. Chem. Chem. Phys. 5 (2003) 1010.
[9] J. Liu, S. Mandel, C.M. Hadad, M.S. Platz, J. Org. Chem. 69 (2004) 8583.
[10] R.E. Wilde, T.K.K. Srinivasan, W. Lwowski, J. Am. Chem. Soc. 93 (1971) 860.
[11] J.H. Teles, G. Maier, Chem. Ber. 122 (1989) 745.
[12] M.E. Sigman, T. Autrey, G.B. Schuster, J. Am. Chem. Soc. 110 (1988) 4297.
[13] M.J. Frisch, G.W. Trucks, H.B. Schlegel, G.E. Scuseria, M.A. Robb, J.R. Cheeseman, J.A. Montgomery Jr., T. Vreven, K.N. Kudin, J.C. Burant, J.M. Millam, S.S. Iyengar, J. Tomasi, V. Barone, B. Mennucci, M. Cossi, G. Scalmani, N. Rega, G.A. Petersson, H.M. Nakatsuji, M. Hada, M. Ehara, K. Toyota, R. Fukuda, J. Hasegawa, M. Ishida, T. Nakajima, Y. Honda, O. Kitao, H. Nakai, M. Klene, X. Li, J.E. Knox, H.P. Hratchian, J.B. Cross, C. Adamo, J. Jaramillo, R. Gomperts, R.E. Stratmann, O. Yazyev, A.J. Austin, R. Cammi, C. Pomelli, J.W. Ochterski, P.Y. Ayala, K. Morokuma, G.A. Voth, P. Salvador, J.J. Dannenberg, V.G. Zakrzewski, S. Dapprich, A.D. Daniels, M.C. Strain, O. Farkas, D.K. Malick, A.D. Rabuck, K. Raghavachari, J.B. Foresman, J.V. Ortiz, Q. Cui, A.G. Baboul, S. Clifford, J. Cioslowski, B.B. Stefanov, G. Liu, A. Liashenko, P. Piskorz, I. Komaromi, R.L. Martin, D.J. Fox, T. Keith, M.A. Al-Laham, C.Y. Peng, A. Nanayakkara, M. Challacombe, P.M.W. Gill, B. Johnson, W. Chen, M.V. Wong, C. Gonzalez, J.A. Pople, Gaussian 03, Revision A.1, Gaussian, Inc., Pittsburgh, PA, 2003.
[14] (a) A.D. Becke, J. Chem. Phys. 98 (1993) 5648;
(b) C. Lee, W. Yang, R.G. Parr, Phys. Rev. B 37 (1988) 785.
[15] (a) J. Labanowski (Ed.), Density Functional Methods in Chemistry, Springer-Verlag, Heidelberg, 1991;
(b) R.G. Parr, Y. Weitao, Density-Functional Theory in Atoms and Molecules, Oxford University Press, New York, 1989;
(c) R. Bauernschmitt, Chem. Phys. Lett. 256 (1996) 454; (d) R. Stratmann, J. Chem. Phys. 109 (1998) 8218;
(e) J.B. Foresman, T.A. Keith, K.B. Wiberg, J. Snoonian, M.J. Frisch, J. Phys. Chem. 100 (1996) 16098;
(f) J. Foresman, J. Phys. Chem. 96 (1992) 135.
[16] (a) J. Tomasi, B. Mennucci, R. Cammi, Chem. Rev. 105 (2005) 2999;
(b) B. Mennucci, E. Cancès, J. Tomasi, J. Phys. Chem. B 101 (1997) 10506;
(c) E. Cancès, B. Mennucci, J. Chem. Phys. 114 (2001) 4744;
(d) J. Tomasi, M. Persico, Chem. Rev. 94 (1994) 2027;
(e) C.J. Cramer, D.J. Truhlar, Chem. Rev. 99 (1999) 2161.
[17] (a) C. Gonzalez, H.B. Schlegel, J. Chem. Phys. 90 (1989) 2154;
(b) C. Gonzalez, H.B. Schlegel, J. Phys. Chem. 94 (1990) 5523.
[18] N.P. Gritsan, H.B. Zhai, T. Yuzawa, D. Karweik, J. Brooke, M.S. Platz, J. Phys. Chem. A 101 (1997) 2833.
[19] J.C. Scaiano, J. Am. Chem. Soc. 106 (1980) 7747.
[20] B.S. Ault, J. Am. Chem. Soc. 100 (1978) 2426.
[21] N. Goldberg, B.S. Ault, Chem. Phys. Lett. 401 (2005) 89.
[22] F. Bottari, E. Nannipieri, M.F. Saettone, M.F. Serafini, J. Med. Chem. 15 (1972) 39.
[23] D.S. Farrier, Arzneim. Forsch. 25 (1975) 813.
[24] P.F. McGarry, C.E. Doubleday Jr., C.-H. Wu, H.A. Staab, N.J. Turro, J. Photochem. Photobiol. A 77 (1994) 109.
[25] S.L. Murov, I. Carmichael, G.L. Hug, Handbook of Photochemistry, M. Dekker, New York, 1993.
[26] H. Lutz, L. Lindquist, Chem. Commun. (1971) 493.
[27] J.N. Crowley, J.R. Sodeau, J. Phys. Chem. 93 (1989) 3100.
[28] J.B. Foresman, Æ. Frisch, Exploring Chemistry with Electronic Structure Methods, 2nd ed., Gaussian, Inc., Pittsburgh, PA, 1996, p. 64.
[29] I.R. Dunkin, Matrix Isolation Techniques: A Practical Approach, Oxford University Press, New York, 1998.
[30] (a) S. Muthukrishnan, S. Mandel, J.C. Hackett, P.N.D. Singh, C.M. Hadad, J.A. Krause, A.D. Gudmundsdottir, J. Org. Chem. 72 (2007) 2757;
(b) P.N.D. Singh, S.M. Mandel, Z. Zhu, R. Franz, B.S. Ault, A.D. Gudmundsdottir, J. Org. Chem. 68 (2003) 7951;
(c) S.M. Mandel, J.A. Krause Bauer, A.D. Gudmundsdottir, Org. Lett. 3 (2001) 523.
[31] (a) P.N.D. Singh, S.M. Mandel, J. Sankaranarayanan, S. Muthukrishnan, M. Chang, R.M. Robinson, P.M. Lahti, B.S. Ault, A.D. Gudmundsdottir, J. Am. Chem. Soc. 129 (2007) 16263;
(b) R.F. Klima, A.V. Jadhav, P.N.D. Singh, M. Chang, C. Vanos, J. Sankaranarayanan, M. Vu, N. Ibrahim, E. Ross, S. McCloskey, R.S. Murthy, J.A. Krause, B.S. Ault, A.D. Gudmundsdottir, J. Org. Chem. 72 (2007) 6372;
(c) J. Sankaranarayanan, L. Bort, J.A. Krause, S.M. Mandel, P. Chen, E.E. Brooks, P. Tsang, A.D. Gudmundsdottir, Org. Lett. 10 (2008) 937.
[32] E. Leyva, M.S. Platz, G. Persy, J. Wirz, J. Am. Chem. Soc. 108 (1986) 3783.